INTERNATIONAL JOURNAL OF REFRIGERATION 35 (2012) 663–675

Available online at www.sciencedirect.com

SciVerse ScienceDirect

journal homepage: www.elsevier.com/locate/ijrefrig

Performance studies on the desiccant packed bed with varying particle size distribution along the bed

A. Ramzy K, Ravikiran Kadoli, T.P. Ashok Babu*

Mechanical Engineering Department, National Institute of Technology Karnataka, Surathkal, Mangalore 575025, India

ARTICLE INFO

Article history:
Received 22 February 2011
Received in revised form
16 November 2011
Accepted 22 November 2011
Available online 6 December 2011

Keywords:
Optimization
Adsorbent
Adsorption
Desorption
Desiccant
Silica gel

ABSTRACT

The transient heat and mass transfer in a desiccant packed bed containing varying particle diameter distribution along the axial direction has been investigated using the pseudo gas controlled approach that considers the heat conduction in the bed. The numerical results of the present model and the experimental data from literature show good agreement with a maximum root of mean square of errors of 3% and 2% for exit air temperature and humidity ratio, respectively. The improvement in the total mass adsorbed and/or reduction in pressure drop has been investigated for various cases of packed bed namely, uniform particle diameter, linear, parabolic and cubic ascending and descending distributions. It has been found that there is a 25.7% reduction in pressure drop with negligible reduction in the total mass adsorbed for a desiccant bed with cubic type particle size distribution when compared to the bed with uniform particle diameter of 1.0 mm. A threshold flow velocity exists below which the total mass adsorbed is independent of particle diameter distribution type.

Etudes sur la performance d'un matelas dispersant avec une distribution de la taille des particules différente selon les emplacements

Mots clés : Optimisation ; Adsorbant ; Adsorption ; Désorption ; Déshydratant ; Gel de silice

1. Introduction

Adsorption cooling cycles and desiccant air dehumidification systems are considered as good alternatives for the commonly used vapor compression cooling systems. It gives the ability to use the waste heat from various applications as well as low grade energy sources like solar energy as a regeneration energy source. Many researchers have investigated the desiccant air dehumidification systems and evaporative cooling systems, Jia et al. (2007), Elsayed et al. (2008), Chung

* *Corresponding author.*
E-mail addresses: ahmed_ara1979@mans.edu.eg (A. Ramzy K), rkkadoli@nitk.ac.in (R. Kadoli), tpashok@rediffmail.com (T.P. Ashok Babu).
0140-7007/$ – see front matter © 2011 Elsevier Ltd and IIR. All rights reserved.
doi:10.1016/j.ijrefrig.2011.11.016

Nomenclature

A	bed cross section area [m^2]
a	volumetric transfer area [m^{-1}]
C	equation constant
c	specific heat [J kg^{-1} K^{-1}]
D	diameter [m]
DP	pressure drop [Pa]
dt	time increment size [sec]
dy	bed length increment size [m]
E	Young's modulus [N m^{-2}]
G	mass flux, ($G = \dot{m}/A$) [kg m^{-2} s^{-1}]
HTR	heat transfer rate [W]
h	enthalpy [J kg^{-1}]
k_h	heat transfer coefficient [W m^{-2} K^{-1}]
k_m	mass transfer coefficient [kg m^{-2} s^{-1}]
L	length of the bed [m]
VMTR	volumetric mass transfer rate [kg s^{-1}]
$\dot{m}$	mass flow rate [kg s^{-1}]
P	pressure [Pa]
Q	heat transfer rate [W]
RH	relative humidity [%]
Re	Reynolds number
r	radius of contact spot [m]
t	time [sec]
v	volume [m^3]
ν	velocity [m s^{-1}]
W	gel water content [kg_w $kg^{-1}_{\text{dry silica gel}}$]
y	axial position [m]

Greek

ε	porosity
ϕ	heat of adsorption [J kg^{-1}]
λ	thermal conductivity [W m^{-1} K^{-1}]
λ_c	conductivity through contact area [W m^{-1} K^{-1}], Eq. (23)
λ'	corrected conductivity [W m^{-1} K^{-1}], Eq. (22)
μ	air dynamic viscosity [N s m^{-2}]
θ	temperature [°C]
ρ	density [kg m^{-3}]
υ	Poisson ratio, Eq. (24)
ω	humidity ratio [kg_υ $kg^{-1}_{\text{dry air}}$]

Subscripts

a	air
b	bed
c	conduction
e	exit value
eff	effective
i	inlet value
min	minimum value
max	maximum value
o	initial condition
p	particle
s	silica gel side
sat	saturation
t	total
υ	vapor
w	water

and Lee (2009), Jeong et al. (2010, 2011), Ruivo et al. (2011), Heidarinejad and Pasdarshahri (2011), White et al. (2011). In these systems, the main function of desiccant wheel is the air dehumidification process. However, it is well known that the desiccant packed bed can be used, with some modifications in the system, for the same purpose of desiccant wheel. Moreover, many researchers have dealt with the adsorption chillers in which the adsorbent bed is the main component of the system, Liu et al. (2005), Maggio et al. (2006), Wang and Chua (2007) and Miyazaki et al. (2010). On the other hand, the sorption systems are widely used in other engineering applications like gas separation processes (Kluson et al., 2000; San et al., 1998) and adsorption of dilute dissolved gases from liquids (Mutlu and Gökmen, 1998). The adsorbent bed is the key component of the sorption systems in which the adsorption and desorption processes take place on the surface of adsorbent particles. These adsorption and desorption processes can be treated as transient heat and mass transfer processes, therefore many researchers have investigated the heat and mass transfer in desiccant beds, Meyer and Weber (1967) modeled theoretically and experimentally the non-isothermal adsorption of methane from a helium stream in packed bed of activated carbon considering the radial heat transfer to the wall of the bed, but the axial heat conduction and moisture diffusion were neglected. Farooq and Ruthven (1990) studied the heat and mass transfer in a desiccant packed bed using a two dimension model. Thermal equilibrium condition was assumed between the gas flow and the desiccant particles. It was found that as the value of dimensionless heat generation increases, the heat effect becomes significant and asymmetry develops. The same was investigated by Kim et al. (2004) for the adsorption of moisture in a packed bed of zeolite-13X to investigate the effect of radial temperature distribution on the adsorption and desorption dynamics. However, it was recommended that the one dimension model is sufficient to predict the performance of the bed. Kafui (1994) considered the effect of intra-particle conduction heat transfer in the bed, and modeled the mass transfer in the bed considering both pore and surface diffusion rates inside the silica gel particles. San and Jiang (1994) analyzed the transient response of two silica gel packed beds arranged in periodic steady state operation using SSR model which was modified to incorporate the effect of fluid friction in the gas phase energy balance equation. Sun and Besant (2005) modeled the moisture and heat transfer in a packed bed of silica gel and concluded that using smaller particles of desiccant (silica gel) increases the moisture transfer rate to the bed. Some other researchers were interested in improving the desiccant bed performance in view to reduce the operating energy requirements and make better utilization of the desiccant material in the bed. In order to reduce the effect of heat of adsorption and improve the bed performance, Majumdar (1998) studied the operation of a composite packed bed dehumidifier in which the desiccant particles were mixed with inert high specific heat particles, Chang et al. (2005) studied the performance of a matrix wherein silica gel particles were pasted on a stainless steel substrates. The particle size was the variable parameter and it

was found that the mass transfer performance of the system is better when thinner consolidated layer made of larger silica gel particles was used. Sircar (2006) used the fact that higher gas flow rates result in an observable increase in the heat transfer rates by forced convection in packed beds to remove the heat of adsorption and obtain isothermal sorption process. Weixing et al. (2008) constructed and tested a cross cooled compact dehumidifier consisting of small channels in which the silica gel particles are glued on its surface and an increase of 12.4% in the moisture removal rate was achieved using the cross cooling for the bed and Rady et al. (2009) proposed a dehumidifying bed made of macro-encapsulated phase change material mixed with silica gel particles, and it was observed that the sudden increase in the system temperature during the adsorption process has been eliminated when the proposed mixture was used. Moreover it was recommended to use a phase change material with a phase change temperature close to the inlet air temperature which can enhance the system performance during the effective first stage of the adsorption process. Awad et al. (2008) showed that with a radial flow desiccant packed bed, better air dehumidification can be achieved with less blowing power requirements. Ramzy et al. (2011) proposed a composite particle to improve desiccant material utilization by increasing the contact area in the packed bed. It was found that the proposed composite particles can increase the total mass adsorbed by 11% and decrease the pressure drop by 60%.

From the forgoing discussion, it is to be concluded that with a view to improve the bed performance the objectives were: reducing the blowing power requirements and increasing the desiccant material utilization. Moreover, an attempt to improve the performance of solid desiccant should include an investigation on the performance of the packed bed when the particle diameter changes. The case of a desiccant packed bed of silica gel particles is selected during this study because of many available literatures for water–silica gel isotherms (Ng et al., 2001; Anderson et al., 1985; Chua et al., 2002; Chakraborty et al., 2009) and the experimental investigations on silica gel packed beds (Pesaran and Mills, 1987b; Sun and Besant, 2005). In the present study, the heat and mass transfer combined with the effects of pressure drop in the vertical desiccant packed bed is modeled. The PGC-model (Pesaran and Mills, 1987a) has been modified to consider the axial conduction heat transfer in the bed which is expected to enhance the model accuracy when desiccant particle diameter is a variable parameter. The modified model is validated with the comparison with the experimental work from literatures: Pesaran and Mills (1987b) and Sun and Besant (2005). The dynamic response of the bed performance due to changing the particle diameter will be investigated and optimization procedure will be presented to include the pressure drop limitations. Also, a new technique of multi-layer bed, wherein particle size changes for each layer is suggested as shown in Fig. 1, as it may improve the heat and mass transfer and/or decrease the pressure drop in the bed. Six types of particle diameter distributions along the bed are considered and compared with the case of using uniform particle diameter.

2. Mathematical modeling

The operation of desiccant packed bed during adsorption and desorption processes includes two transfer processes. The first is mass transfer, referred to as adsorption process. During this process the adsorbate molecules are transferred from the bulk gas flow to the desiccant surface due to adsorbate vapor pressure difference, and the mass transfer direction is inversed

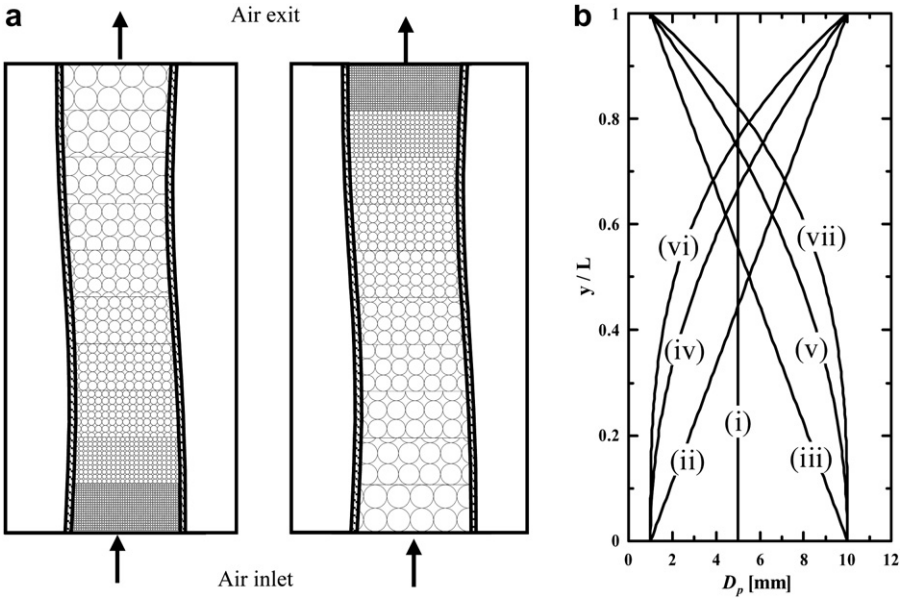

Fig. 1 – (a) General concept of desiccant bed with varying particle diameter distribution along the bed length. (b) various distributions of desiccant particle diameter along the bed, i – uniform, ii, iii – linear ascending and descending, iv, v – parabolic ascending and descending and vi, vii- cubic ascending and descending respectively.

during the desorption process when the desiccant is being reactivated. During the adsorption process, the adsorbate molecules on the desiccant surface start to condense in the pores, and an amount of phase change energy is released in the form of heat of adsorption which causes an increase in the desiccant temperature. The second transfer process is the heat transfer from the desiccant to/from the bulk gas flow. Considering that the adsorbate vapor pressure on the desiccant surface is highly influenced by the desiccant temperature and the adsorbate content on the desiccant, the heat of adsorption is dependant on the mass transfer rate which, in turns, is influenced by the adsorbate vapor pressure on the desiccant surface. Hence, the problem of adsorption and desorption has to be treated as a coupled transient heat and mass transfer case. Fig. 2 shows the incremental volume of the packed bed where the air condition (θ_a and ω_a) is transient and changing along axial direction (y-axis) and the bed condition are θ_s and W which also are transient and changing along the axial direction. In the following derivation the adsorbate and energy balances will be applied to the gas and solid phase to develop the modified PGC-model. Applying the adsorbate balance in the gas flow stream in the bed:

$$\dot{m}_a\omega_a(y) - \dot{m}_a\omega_a(y+dy) = \varepsilon\rho_a\frac{1}{2}\frac{\partial}{\partial t}(\omega_a(y)+\omega_a(y+dy))\,dv + (1-\varepsilon)\rho_s\frac{\partial W}{\partial t}dv \quad (1)$$

neglecting the second order differentiation terms $(\partial^2\omega/\partial t\partial y)$, Eq. (1) can be rearranged as

$$-G_a\frac{\partial\omega_a}{\partial y} = \varepsilon\rho_a\frac{\partial\omega_a}{\partial t} + (1-\varepsilon)\rho_s\frac{\partial W}{\partial t} \quad (2)$$

Where G_a is the mass flux of air. Applying the adsorbate balance in the solid phase:

$$(1-\varepsilon)\rho_s\frac{\partial W}{\partial t}dv = k_m a\left(\frac{\omega_a(y)+\omega_a(y+dy)}{2.0} - \omega_s\right)dv \quad (3)$$

Where k_m is the mass transfer coefficient, a is the volumetric specific area and ω_s is the equilibrium adsorbate content on the surface of the desiccant material and is calculated using the desiccant isotherms shown in Fig. 3 along with the particle temperature (θ_s). Rearranging Eq. (3) the adsorbate balance in the solid phase gives:

$$\frac{\partial W}{\partial t} = \frac{k_m a}{(1-\varepsilon)\rho_s}\left(\omega_a + \frac{1}{2}\frac{\partial\omega_a}{\partial y} - \omega_s\right) \quad (4)$$

Substituting Eq. (4) into Eq. (2) and rearranging:

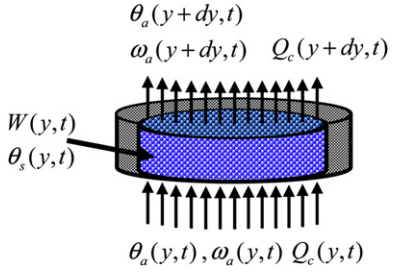

Fig. 2 – The desiccant bed physical model as an incremental volume on which various system parameters are explained.

$$\frac{\partial\omega_a}{\partial t} + \left(\frac{G_a}{\varepsilon\rho_a} + \frac{1}{2}k_m a\right)\frac{\partial\omega_a}{\partial y} = \frac{k_m a}{\varepsilon\rho_a}(\omega_s - \omega_a) \quad (5)$$

Applying the energy balance in the gas flow stream:

$$\begin{aligned}\dot{m}_a h_a(y) - \dot{m}_a h_a(y+dy) =& k_h a\left(\frac{1}{2}(\theta_a(y)+\theta_a(y+dy)) - \theta_s\right)dv \\ &+ \rho_a\varepsilon\frac{1}{2}\frac{\partial(h_a(y)+h_a(y+dy))}{\partial t}dv \\ &- c_v(1-\varepsilon)\rho_s\frac{\partial W}{\partial t} \\ &\times\left(\frac{1}{2}(\theta_a(y)+\theta_a(y+dy)) - \theta_s\right)dv\end{aligned} \quad (6)$$

where, k_h is the convective heat transfer coefficient in the bed. Rearranging Eq. (6)

$$\begin{aligned}&\frac{\partial\theta_a}{\partial t} + \left(\frac{1}{2}\left(\frac{c_v(1-\varepsilon)\rho_s}{c_a\varepsilon\rho_a}\frac{\partial W}{\partial t} - \frac{k_h a}{\rho_a c_a\varepsilon}\right) - \frac{G_a}{\rho_a\varepsilon}\right)\frac{\partial\theta_a}{\partial y} \\ &= \left(\frac{k_h a}{\rho_a c_a\varepsilon}\frac{c_v(1-\varepsilon)\rho_s}{c_a\varepsilon\rho_a}\frac{\partial W}{\partial t}\right)(\theta_a - \theta_s)\end{aligned} \quad (7)$$

Applying the energy balance equation for the solid phase:

$$\begin{aligned}(1-\varepsilon)\rho_s c_s\frac{\partial\theta_s}{\partial t}dv =& Q_c(y) - Q_c(y+dy) + (1-\varepsilon)\rho_s\phi\frac{\partial W}{\partial t}dv \\ &+ k_h a\left(\frac{\theta_a(y)+\theta_a(y+dy)}{2.0} - \theta_s\right)dv\end{aligned} \quad (8)$$

Where Q_c is the heat transfer rate by conduction $(Q_c = -\lambda_{eff}A(\partial\theta/\partial y))$. Rearranging Eq. (8) the solid phase energy balance is as follows:

$$\frac{\partial\theta_s}{\partial t} - \frac{\lambda_{eff}}{(1-\varepsilon)\rho_s c_s}\frac{\partial^2\theta}{\partial y^2} = \frac{k_h a}{(1-\varepsilon)\rho_s c_s}\left(\theta_a + \frac{1}{2}\frac{\partial\theta_a}{\partial y} - \theta_s\right) + \frac{\phi}{c_s}\frac{\partial W}{\partial t} \quad (9)$$

In Eq. (9), the parameter ϕ represents the heat of sorption released or absorbed during adsorption or desorption processes, respectively. The sorption heat is a function of the silica gel water content and has been presented by Pesaran and Mills (1987a, b) as follows,

$$\phi = \begin{cases} 3500.0 - 13400.0\times W & W \le 0.05 \\ 2950.0 - 1400.0\times W & W > 0.05 \end{cases} \quad (10)$$

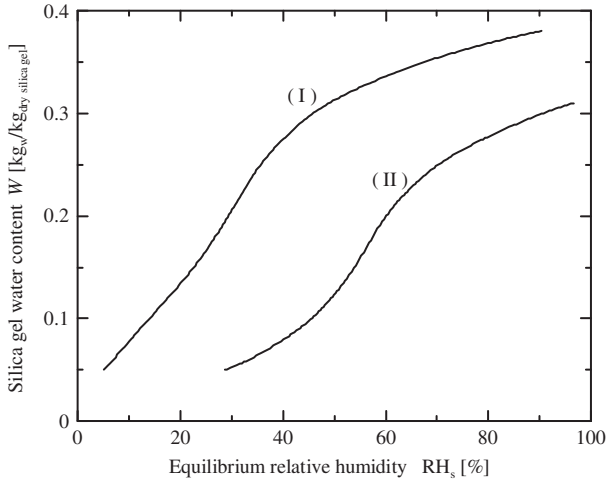

Fig. 3 – Water–silica gel isotherms (I and II) as presented in Pesaran and Mills (1987b) and Sun and Besant (2005), respectively.

The density of silica gel used by Pesaran and Mills (1987a, b) and Sun and Besant (2005) are 1128.0 and 2400.0 kg m^{-3}, respectively. The specific heats of silica gel and humid air are calculated as follows (Pesaran and Mills, 1987a):

$$c_s = 4186.0 \times W + 921.0 \tag{11}$$

$$c_a = 1884.0 \times \omega_a + 1004.0(1 - \omega_a) \tag{12}$$

Pesaran and Mills (1987b) used the equilibrium isotherm (I) of water–silica gel by fitting the data provided by the manufacturer as follows;

$$RH_s = 100(0.0078 - 0.05759W + 24.16554W^2 - 124.478W^3 + 204.226W^4) \tag{13}$$

And for the silica gel used by Sun and Besant (2005), the isotherm (II) was generated by curve fitting the experimental data of moisture adsorption capacity measurement of silica gel particles at the end of each experimental run and presented as follows:

$$RH_s = 100(-0.0173 + 7.932W - 40.233W^2 + 80.192W^3) \tag{14}$$

The plots for Eqs. (13) and (14) are presented in Fig. 3. Using the calculated equilibrium relative humidity (RH_s) and the bed temperature (θ_s), the equilibrium moisture content of the air adjacent to the particle surface (ω_s) is calculated as follows (Pesaran and Mills, 1987a):

$$\omega_s = \frac{0.622RH_s \times P_{sat}(\theta_s)}{P_{tot} - 0.378RH_s \times P_{sat}(\theta_s)} \tag{15}$$

The bed porosity has been taken as 0.3. The convective heat and mass transfer coefficients in cylindrical packed bed of spherical particles are calculated using the following relations (Pesaran and Mills, 1987a):

$$k_h = 0.683\rho_a v c_a Re^{-0.51} \tag{16}$$

$$k_m = 0.704\rho_a v Re^{-0.51} \tag{17}$$

3. Bed effective conductivity

The effective conductivity of packed beds of dry and moist silica gel particles have been investigated by Gurgel et al. (2001) and Bjurstrom et al. (1984). In the present study, the effective bed conductivity models discussed in Bjurstrom et al. (1984) will be put to practice. The experimental data for the conductivity of silica gel particle (λ_s) variation with silica gel particle water content (W) is fitted with a fifth order polynomial (Eq. (18)) with the regression constants as $a_0 = 0.3898455711$, $a_1 = 1.764096737$, $a_2 = -17.96241259$, $a_3 = 174.6678322$, $a_4 = -731.1188811$ and $a_5 = 1061.538462$. Three models of effective conductivity λ_{eff} are used namely, geometric mean model (Eq. (19)), Russell's model (Eq. (20)), and stochastic model (Eqs. (21)–(24)).

$$\lambda_s = a_0 + a_1W + a_2W^2 + a_3W^3 + a_4W^4 + a_5W^5 \tag{18}$$

$$\lambda_{eff} = \lambda_a^{\varepsilon}\lambda_s^{1-\varepsilon} \tag{19}$$

$$\lambda_{eff} = \frac{\lambda_a\lambda_s(1-\varepsilon)^{2/3} + \lambda_a^2\left(1 - (1-\varepsilon)_s^{2/3}\right)}{\lambda_s(1-\varepsilon)^{2/3} - \lambda_s(1-\varepsilon) + \lambda_a\left(2 - (1-\varepsilon)^{2/3} + \varepsilon\right)} \tag{20}$$

$$\lambda_{eff} = \lambda_a\varepsilon^2 + \lambda_s'(1-\varepsilon)^2 + \frac{4\lambda_s'\lambda_a\varepsilon(1-\varepsilon)}{\lambda_s' + \lambda_a} \tag{21}$$

Where λ_s' is the corrected form of silica gel conductivity to consider the contact resistances in the packed bed and is calculated as:

$$\frac{1}{\lambda_s'} = \frac{1}{\lambda_s} + \frac{3}{3\lambda_c + 100\lambda_a} \tag{22}$$

Where λ_c is the conductivity through the contact area and can be calculated as

$$\lambda_c = \lambda_s\left(\frac{1-\varepsilon}{0.75}\right)^{\frac{1}{3}}\left(\frac{470\pi r^2}{D_p^2} + \frac{7P_3^{\frac{2}{3}}}{1500}\right) \tag{23}$$

Where r is the radius of the contact spot which can be calculated as follows,

$$r = 0.465D_p\left(\frac{1-v^2}{E}\frac{\rho_p L}{1-\varepsilon}\right)^{\frac{1}{3}} \tag{24}$$

Where, v is the Poisson ratio and E is Young's modulus and following Bjurstrom et al. (1984) work, these values are taken as 0.25 and 5.5×10^{10} [N m^{-2}] respectively.

4. Effects of particle diameter

The particle diameter is affecting many parameters which greatly affects the system performance, namely heat transfer coefficient, mass transfer coefficient, and pressure drop. For the same velocity of air flow, the convective mass and heat transfer rates can be expressed as follows:

$$VMTR = k_m a(\omega_a - \omega_s) \tag{25}$$

Where the relation for mass transfer coefficient (k_m) and volumetric specific area (a) are calculated as:

$$k_m = CRe^n \tag{26}$$

$$a = \frac{6(1-\varepsilon)}{D_p} \tag{27}$$

Where $n = -0.51$ when PGC model is used (Pesaran and Mills, 1987a). Substituting Eqs. (26) and (27) into Eq. (25) and replacing Reynolds number as $Re = \rho v D_p/\mu$ the following proportionalities can be derived.

$$(VMTR \text{ and } VHTR)\alpha\left(\frac{1}{D_p}\right)^{\frac{3}{2}} \tag{28}$$

And the pressure drop in the bed (DP) is calculated using Ergun's equation quoted in Sodre and Parise (1998) as follow:

$$DP = 150\frac{(1-\varepsilon)^2}{\varepsilon^3}\mu\frac{v}{D_p^2} + 1.75\frac{(1-\varepsilon)}{\varepsilon^3}\rho_a\frac{v^2}{D_p} \tag{29}$$

From Eq. (29) it can be seen that the proportionality relation relating the pressure drop in the packed bed and the particle diameter can be written as:

$$DP\alpha D_p^{-2} \tag{30}$$

Investigating Eqs. (28) and (30), two facts can be stated, first, the mass and heat transfer rates are increasing when particle diameter decreases due to the increase of mass transfer area and specific surface area of the bed. On the other hand, another fact brought to light is that when particle diameter decreases, the pressure drop increases for the same air flow velocity. Combining these two facts and the disadvantages of the packed bed listed by Awad et al. (2008), and Hamed et al. (2010) which includes that the leading layers of the packed bed are utilized effectively during adsorption processes and the trailing edges are weakly utilized and add more pressure drop in the system, a modified configuration of the desiccant packed bed could be obtained. In view of the desiccant packed bed constructed with a well defined particle diameter distribution along the bed, the probable expected operational performance and outcomes would be:

1. Using smaller particle diameter in the trailing layers will enhance the heat and mass transfer in these layers, and it should be noted that the pressure drop will increase with this modification.
2. Using bigger particle diameter in the trailing layers will decrease the pressure drop in the bed, and this will not reduce the adsorption rate significantly because these layers do weakly contribute in the adsorption process compared to the leading layers.

During this work, the desiccant bed is considered to have linear, parabolic and cubic distributions of particle diameter so as to optimize the total mass adsorbed and pressure drop in the bed which is translated to a savings in the required blowing power in the system. Both cases of ascending and descending distributions are considered as shown earlier in Fig. 1(a and b). Eqs. (31) and (32) list the ascending and descending linear ($k = 1$), parabolic ($k = 2$) and cubic ($k = 3$) particle diameter distributions respectively.

$$\text{Ascending distributions}: \quad D_p(y) = D_{pmin} + \left(\frac{y}{L}\right)^k (D_{pmax} - D_{pmin}) \tag{31}$$

$$\text{Descending distributions}: \quad D_p(y) = D_{pmax} + \left(\frac{y}{L}\right)^k (D_{pmax} - D_{pmin}) \tag{32}$$

5. Numerical model and validation

Eqs. (4), (5), (7) and (9) are the mathematical model of heat and mass transfer for the adsorption and desorption processes in a desiccant packed bed. The initial condition of the bed is defined as the initial state of the desiccant material in the bed ($W(y,t) = W_o$ and $\theta_s(y,t=0) = \theta_{so}$) and are used for Eqs. (4) and (9). The boundary conditions for Eqs. (5) and (7) are the inlet air condition ($\omega_a(y=0,t) = \omega_{ai}$ and $\theta_a(y=0,t) = \theta_{ai}$). The numerical results have been calculated using the finite difference method – Crank–Nicholson scheme which is unconditionally stable. During the numerical solution the bed is divided to 100 bed length steps, and the time increment used is 0.1 s. The discretized equations for the differential Eqs. (4), (5), (7) and (9) are listed in Eqs. (33)–(37), respectively.

$$W_j^{n+1} = W_j^n + \frac{a_j dt\left(k_{m_j}^{n+1} + k_{m_j}^n\right)}{2(1-\varepsilon)\rho_s} \times \left(\frac{w_{a_j}^{n+1} + w_{a_j}^n}{2} + \frac{w_{a_{j+1}}^{n+1} - w_{a_j}^{n+1} + w_{a_{j+1}}^n - w_{a_j}^n}{4dy} - \frac{\omega_{s_j}^{n+1} + \omega_{s_j}^n}{2}\right) \tag{33}$$

$$\omega_{a_j}^{n+1} = \omega_{a_j}^n - \left(\frac{G_a dt}{\varepsilon\rho_a} + \frac{a_i dt\left(k_{m_j}^{n+1} + k_{m_j}^n\right)}{4}\right) \times \frac{\left(\omega_{a_{j+1}}^{n+1} + \omega_{a_{j+1}}^n - \omega_{a_j}^{n+1} - \omega_{a_j}^n\right)}{2dy} + \frac{\left(k_{m_j}^{n+1} + k_{m_j}^n\right) a_j dt}{4\varepsilon\rho_a} \times \left(\omega_{s_j}^{n+1} + \omega_{s_j}^n - \omega_{a_j}^{n+1} - \omega_{a_j}^n\right) \tag{34}$$

$$\theta_{a_j}^{n+1} = \theta_{a_j}^n + \left(\frac{G_a dt}{2\rho_a \varepsilon dy} + \frac{\psi_j^n dt}{4dy}\right)\left(\theta_{a_{j+1}}^{n+1} + \theta_{a_{j+1}}^n - \theta_{a_j}^{n+1} - \theta_{a_j}^n\right) + \frac{\psi_j^n dt}{2}\left(\theta_{a_j}^{n+1} + \theta_{a_j}^n - \theta_{s_j}^{n+1} - \theta_{s_j}^n\right) \tag{35}$$

where ψ_j^n is calculated as

$$\psi_j^n = \frac{\left(k_{h_j}^{n+1} + k_{h_j}^n\right) a_j}{\rho_a\left(c_{a_j}^{n+1} + c_{a_j}^n\right)\varepsilon} - \frac{2c_v\rho_s(1-\varepsilon)}{\rho_a\left(c_{a_j}^{n+1} + c_{a_j}^n\right)\varepsilon}\frac{W_j^{n+1} - W_j^n}{dt} \tag{36}$$

$$\theta_{s_j}^{n+1} = \theta_{s_j}^n + \frac{\left(\lambda_{eff_j}^{n+1} + \lambda_{eff_j}^n\right) dt}{2(1-\varepsilon)\rho_s\left(c_{s_j}^{n+1} + c_{s_j}^n\right) dy^2} \times \left(\theta_{s_{j+1}}^{n+1} + \theta_{s_{j+1}}^n - 2\theta_{s_j}^{n+1} - 2\theta_{s_j}^n + \theta_{s_{j-1}}^{n+1} + \theta_{s_{j-1}}^n\right) + \frac{\left(\phi_j^{n+1} + \phi_j^n\right)}{\left(c_{s_j}^{n+1} + c_{s_j}^n\right)}\left(W_j^{n+1} - W_j^n\right) + \frac{a_j\left(k_{h_j}^{n+1} + k_{h_j}^n\right) dt}{2(1-\varepsilon)\left(c_{s_j}^{n+1} + c_{s_j}^n\right)\rho_s} \times \left(\theta_{a_j}^{n+1} - \theta_{s_j}^{n+1} + \theta_{a_j}^n - \theta_{s_j}^n + \frac{1}{2dy}\left(\theta_{a_{j+1}}^{n+1} + \theta_{a_{j+1}}^n - \theta_{a_j}^{n+1} - \theta_{a_j}^n\right)\right) \tag{37}$$

To investigate the model validation for the prediction of bed performance during adsorption as well as desorption process, the experimental data reported by Pesaran and Mills (1987b) and Sun and Besant (2005) have been used. The input data for the experimental runs are furnished in Table 1.

6. Results and discussion

6.1. *Bed conductivity*

The silica gel conductivity is measured experimentally by Bjurstrom et al. (1984) for different values of gel water content (W), the experimental values of silica gel conductivity (λ_s) are shown in Fig. 4 as filled circles, it can be seen that increasing

Table 1 – Bed and flow conditions for experiments (Pesaran and Mills, 1987a, b; Sun and Besant, 2005).

Run	Ref.	Process	D_b mm	D_p mm	L cm	W_o kg_w $kg^{-1}_{dry\ silica\ gel}$	θ_{so} °C	θ_{ai} °C	w_{ai} kg_v $kg^{-1}_{dry\ air}$	v m s^{-1}	t h
1	28	Ads	130	3.88	7.75	0.0417	23.3	23.3	0.01	0.21	0.5
2	28	Ads	130	2.54	6.5	0.041	24.7	24.7	0.0106	0.39	0.5
3	28	Ads	130	5.2	5.0	0.0668	25.6	25.6	0.01093	0.4	0.5
4	28	Des	130	5.2	5.0	0.37	23.8	23.5	0.009	0.65	0.33
5	36	Ads	102.6	1.0	8.0	0.004	22.0	22.0	0.01157	0.0708	10

Ads: adsorption, Des: desorption, Ref: reference.

the silica gel water content the conductivity is increasing. This is due to the increase of moisture in the pores which will reduce the thermal resistance of the pores in the particle. Thermal conductivity of air (λ_a) is assumed to be constant for the working temperature range of (10–100 °C) as referred from Incropera et al. 2007. The effective bed conductivity (λ_{eff}) which is needed for the modeling of heat transfer in the solid phase of the bed (Eq. (9)) are calculated using geometric mean model (Eq. (19)), Russell's model (Eq. (20)), and stochastic model (Eq. (21)). The predicted effective bed conductivity is compared with the experimental values as shown in Fig. 4. It can be observed that for water content range of 0.0–0.35, Russel's model yields higher estimation for λ_{eff} with a mean square root of error of 42.4%, and Stochastic model has lower estimation with a mean square root of errors of 19.1%. On the other hand, a good agreement is observed when geometric mean is used and a mean square root of errors of 9.7% is recorded. Therefore, geometric mean model has been used for the effective bed conductivity during the modeling of heat and mass transfer in the silica gel packed bed.

6.2. *Model validation*

The heat and mass transfer model (Eqs. (4), (5), (7) and (9)) have been solved numerically and the input data listed in Table 1 are used to predict the bed operation during adsorption and desorption processes. A comparison between the experimental data and the present model is evaluated and presented graphically. Fig. 5 shows the exit air humidity ratio versus the relative time for runs number 1, 2 and 3. It can be observed that the humidity is minimum as the operation starts and increases sharply and gradually depending on the bed operating parameters. The same holds true for exit air temperature, Fig. 6, until the exit air attains a maximum temperature. Because of high adsorption rates during the initial times, the adsorption heat generated increases the bed temperature sharply, and consequently the flowing air is heated by means of convective heat transfer. With this increase in the system temperature, the ability of the bed to adsorb moisture decreases, and the system continues adsorption at a rate limited by heat and mass transfer rates. For the remaining period of the process, water vapor adsorption from air continues and increases the water content of the bed, which gradually decreases the bed ability for adsorption. Therefore, the adsorption rate decreases gradually, and the dehumidified air acts as a cooling fluid which gradually has lower temperature as shown in Figs. 5 and 6.

Fig. 7 shows the experimental results of air temperature at axial position of the bed of ($y/L = 0.5$) for a long time adsorption operation reported by Sun and Besant (2005) along with the theoretical results of this study. It can be seen that the adsorption process is continuing for long time but with very low adsorption rates. Fig. 8 shows the variation of exit air humidity and exit air temperature for the desorption process for the experimental run number 4. In this process a very dry air is used for regeneration (pressure swing or heatless

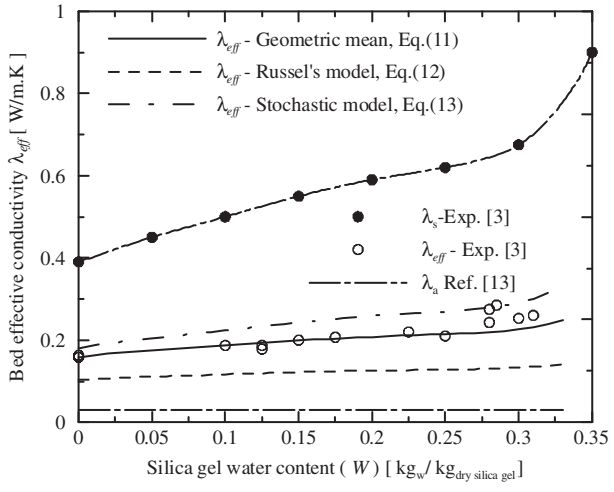

Fig. 4 – Effective bed thermal conductivity using geometric mean model, Russell's model, and stochastic model.

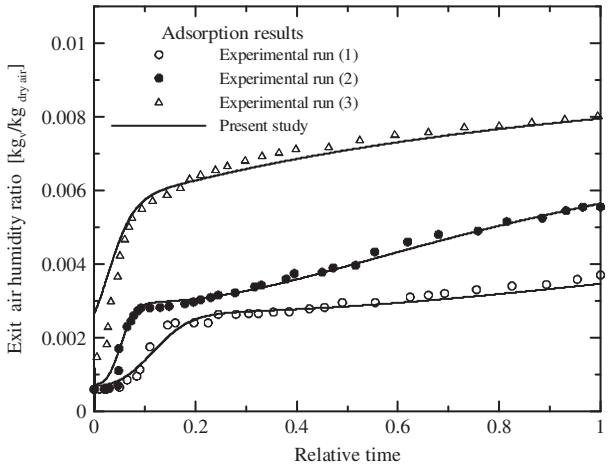

Fig. 5 – Theoretical results and experimental data (Pesaran and Mills, 1987a, b) for exit air humidity ratio (ω_{ae}) during adsorption processes (Runs 1–3).

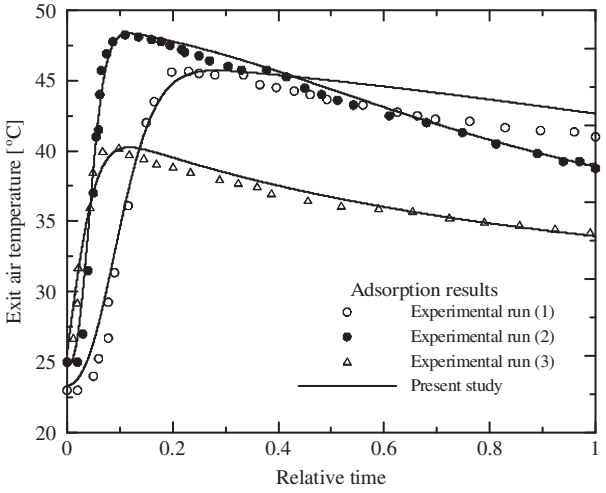

Fig. 6 – Theoretical results and experimental data (Pesaran and Mills, 1987a, b) for exit air temperature (θ_{ae}) during adsorption processes (Runs 1–3).

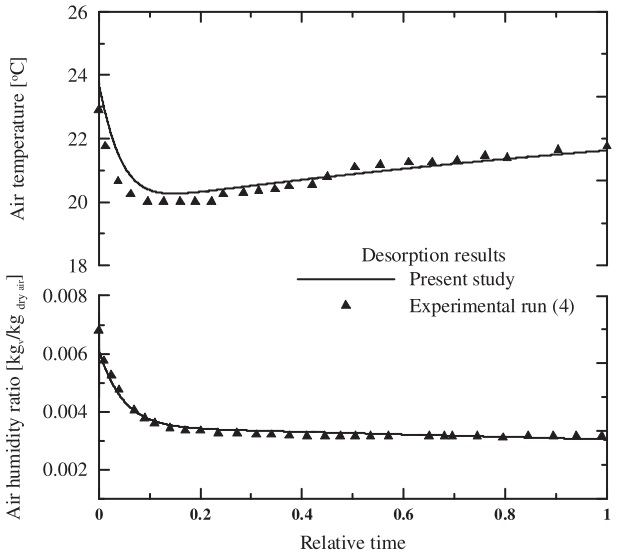

Fig. 8 – Theoretical results and experimental data for exit air temperature (θ_{ae}) and humidity ratio (ω_{ae}) during desorption processes (Run 4).

desorption process). During heatless desorption process the heat required for the water molecules to transfer from liquid phase inside the pores to vapor in the air is extracted from the bed particles therefore the bed temperature reduces during desorption process. As the particles have high water content in the beginning of the desorption process, desorption rate is maximum. With progressing in time, the bed temperature decreases sharply and consequently desorption rate decreases. The regeneration air loses its heat content to the bed by convection and takes the moisture off, this operation results in the high humidity ratio and low temperature at the exit (Fig. 8). The desorption process afterward is limited by the heat transfer from the regeneration air to the bed and the bed water content which is gradually decreasing, then the air temperature is gradually increasing to its inlet temperature and the humidity ratio is decreasing to its inlet value. It can be observed that there is a good agreement between the theoretical results for the system dynamic parameters during the bed operation for the case of short time processes and long time processes with respect to experimental data.

In the following subsections the validated theoretical model has been used for investigating the effect of particle size on the performance of the silica gel packed bed during adsorption operation. Also, the performance of the proposed layered silica gel packed bed with varying particle diameter along the bed has been investigated theoretically. It should be noted that the silica gel density of 1128.0 kg/m^3, bed porosity is 0.3, the isotherm-I (Eq. (13)) and the sorption heat, ϕ (Eq. (10)) have been used through the theoretical investigations.

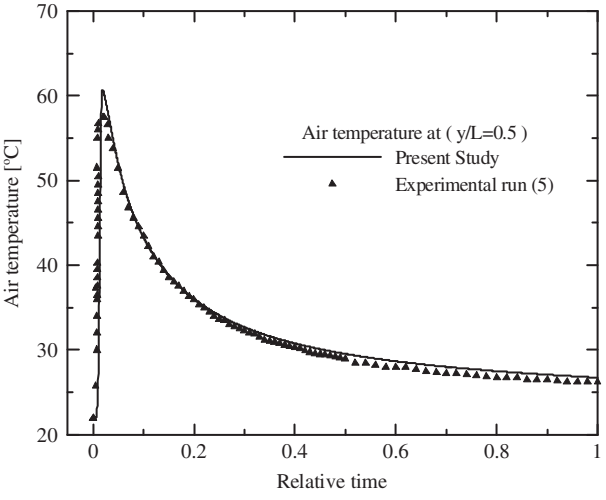

Fig. 7 – Theoretical results and experimental data for air temperature ($\theta_a(y = L/2)$) during adsorption processes (Run 5).

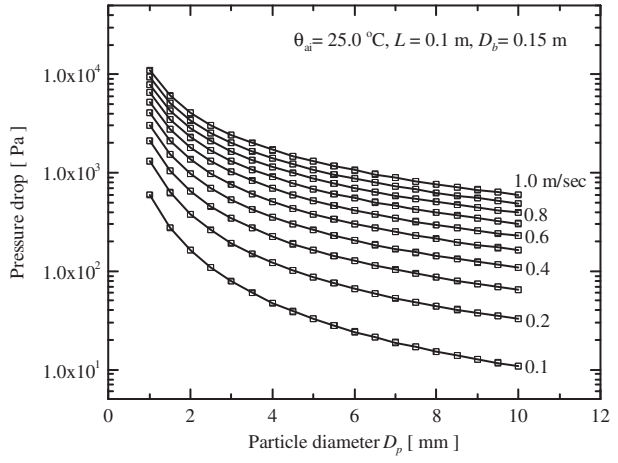

Fig. 9 – Pressure drop in the desiccant bed using different particle diameters (1.0–10.0 mm) at various flow velocities (0.1–1.0 m s^{-1}).

6.3. *Performance of packed bed with axial distribution of uniform particle diameter*

The effect of particle diameter on the pressure drop in the packed bed is shown in Fig. 9. When the particle diameter and/or flow velocity is changed a wide range of pressure drop in the bed is obtained therefore a logarithmic scale has been used for the pressure drop axis. Generally at a specified particle diameter, it can be observed that when the flow velocity increases the pressure drop increases. The same observation can be extracted from Eq. (29) as $(DP\alpha v^2)$.

In addition, the proportionality relation between pressure drop and the particle diameter (Eq. (30)) is observed to be achieved in the Fig. 9, where the increase in the particle diameter decreases the available contact area between the flow and the desiccant particles, consequently the friction losses are reduced. For example, for velocity of 0.1 m s^{-1}, the pressure drop reduces from 600 Pa to 11 Pa (98% reduction) when the particle diameter increases from 1.0 mm to 10.0 mm, and for velocity of 1.0 m s^{-1}, the pressure drop reduces from 11,000 Pa to 600 Pa (94.5% reduction) when the particle diameter increases from 1.0 mm to 10.0 mm. However, it should be noted that the increase/decrease in particle diameter is affecting the values of adsorption rates which will be discussed later.

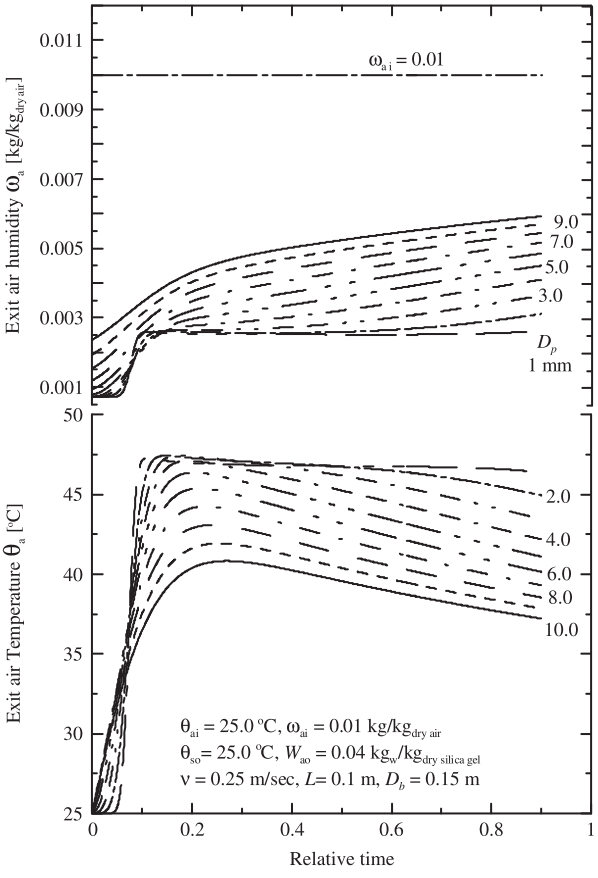

Fig. 10 – Transient variation of exit air humidity ratio and temperature for adsorption process using desiccant beds using different particle diameters (1.0–10.0 mm) at flow velocity (0.25 m s^{-1}).

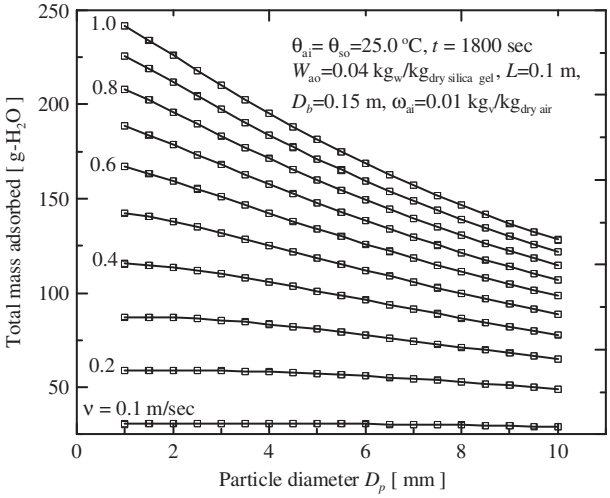

Fig. 11 – Variation of total mass adsorbed during adsorption process in desiccant beds using different particle diameters (1.0–10.0 mm) at various flow velocities (0.1–1.0 m s^{-1}).

The effect of particle diameter on the bed operation is presented in Fig. 10. The bed operation is predicted theoretically for particle diameters of 1.0–10.0 mm. The input data for the run are presented on Fig. 10. It can be observed that minimum exit air humidity ratio is achieved when particle diameter of 1.0 mm is used and the highest is achieved using particles diameter of 10.0 mm. This can be explained by the proportionality relation (Eq. (25)) and by the severe increase in the available specific area for heat and mass transfer when the particle diameter decreases. Also, it can be observed that the trend of the exit air temperature and humidity ratio is slightly changing when the particle diameter changes. For the smaller diameter particles, a sharp increase in the humidity ratio and temperature is observed which can be attributed to the higher adsorption rates at the start period which in turns releases high amount of adsorption heat. On the other hand, for larger particles the increase in exit air humidity takes place gradually because of lower adsorption rates. In addition, it can be observed that the air temperature is higher for smaller particles due to the higher adsorption rates.

The total mass of water adsorbed by the bed during the adsorption process is calculated and plotted in Fig. 11 for various velocities and different particle diameters. It can be observed that for small flow velocity ($v < 0.25$ m s^{-1}) the total mass adsorbed can be considered independent of the particle diameter. And for higher flow velocities, the total mass of water adsorbed is increasing significantly with the decrease in the particle diameters. On the other hand, with smaller particle diameter bed, the pressure drop increases which is a draw back. Fig. 12 shows both pressure drop and total mass adsorbed at a flow velocity of 0.25 m s^{-1} with the variation of particle diameter. It can be observed that decreasing the particle diameter by less than 3.0 mm the total mass adsorbed is slightly increasing and the pressure drop is significantly increasing. Therefore, such a kind of figure like Fig. 12 can be used for optimization of desiccant packed bed design.

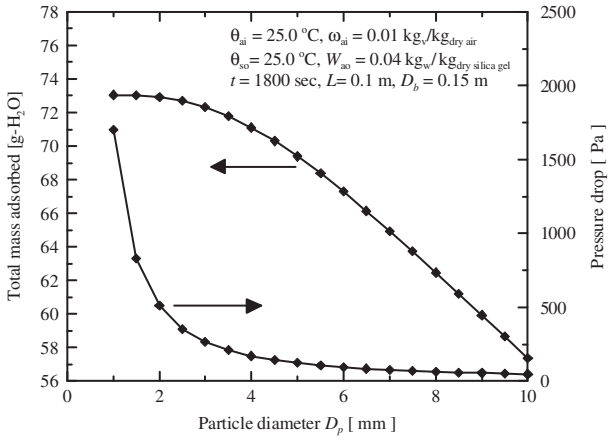

Fig. 12 – Optimization of particle diameter using the variation of total mass adsorbed and pressure drop during adsorption process in desiccant beds at flow velocity (0.25 m s^{-1}).

6.4. *Layered bed of different particle diameter*

At the end of the adsorption process presented in Fig. 10, the axial distribution of the water content of the bed has been extracted from the theoretical results for various uniform particle diameters and is shown in Fig. 13. It can be observed that the water content of the leading layers of the bed is always higher than that of the trailing layers of the bed. However, the difference in the bed water content along the axial direction in the bed is higher for beds with smaller uniform particle diameter. A higher adsorption rates are obtained at the leading layers because of both high mass transfer potential and high specific mass transfer area. Consequently, the air reaching the trailing layers is dry and hot which increases the trailing layers temperature and reduces its ability for adsorption. For the specified operating conditions shown in Fig. 13, it can be observed that the bed water content is very less starting from the region of (y/L = 0.3 to 0.4) indicating the weak utilization of the desiccant material in this portion of the bed. Moreover, the pressure drop in this part of the bed is considered as more burden on the blowing system. It should also be noted that for higher flow rates the weakly utilized portion of the bed is smaller.

The constituents of the bed namely, varying particle diameter as proposed in this work is expected to eliminate the pressure drop in the poorly utilized portion of the bed by using bigger size particles. The same can be used for enhancing the bed adsorptivity by using smaller particles in the trailing layers of the bed. Fig. 14 shows the total mass of water adsorbed during adsorption process at various velocities for seven cases, namely a) uniform particle diameter of 1.0 mm, b) linear ascending distribution, c) linear descending distribution, d) parabolic ascending distribution, e) parabolic descending distribution, f) cubic ascending and g) uniform particle diameter of 10.0 mm. The maximum and minimum particle diameters in the bed with ascending and descending distributions are specified as 1.0 mm and 10.0 mm. From Fig. 14 it can be seen that highest total mass adsorbed is achieved by the bed through the use of uniform particle diameter of 1.0 mm which provides the highest specific area for heat and mass transfer. Then the cubic ascending, parabolic and linear ascending distributions which provide high specific area at the leading layers of the bed where the potential for mass transfer is a maximum. Minimum total mass of water adsorbed is achieved by the beds using uniform particle diameter of 10.0 mm which can be enhanced by using smaller particle diameters at the trailing layers of the bed. From Fig. 14, it can be observed that for linear and parabolic descending distributions the total mass adsorbed is enhanced when compared with that of the bed using uniform particle diameter of 10.0 mm. In addition, it can be observed that the difference in the total mass adsorbed by the uniform particle diameter distribution and that by cubic distribution is very

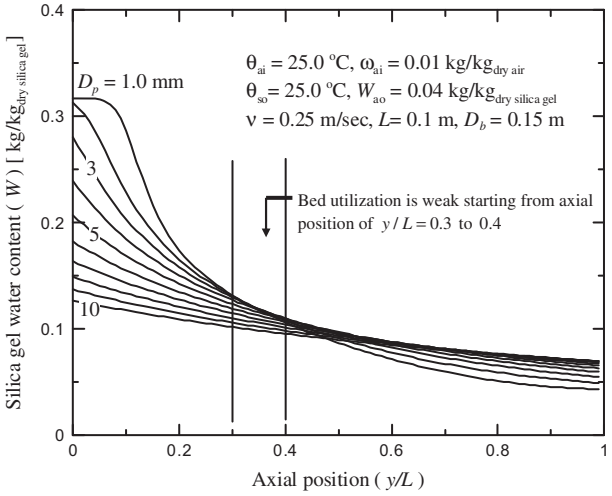

Fig. 13 – Axial distribution of silica gel water content (W) at the end of adsorption process using desiccant beds of different particle diameters (1.0–10 mm) at flow velocity (0.25 m s^{-1}).

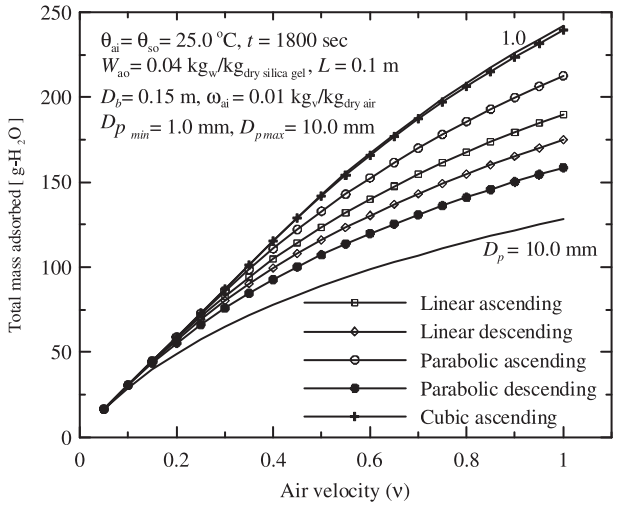

Fig. 14 – The variation of total mass adsorbed at various velocities (0.05–1.0 m s^{-1}) for various particle diameter distributions in the desiccant bed.

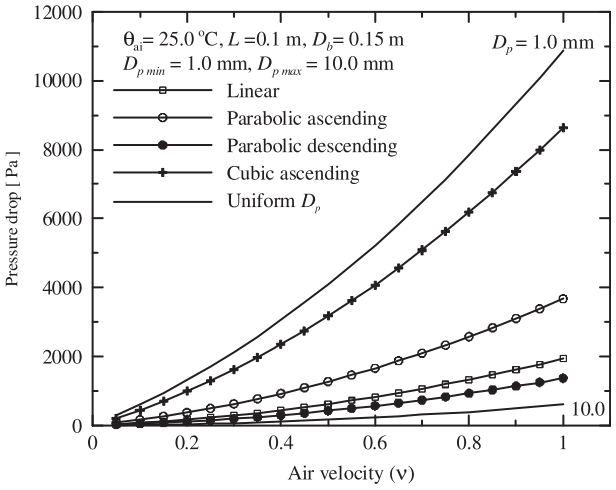

Fig. 15 – Pressure drop in beds using uniform particle diameters and beds with varying particle diameter distributions at various flow velocities (0.05–1.0 m s^{-1}).

small, and for flow velocity ($v < 0.25$ m s^{-1}) the difference in the total mass adsorbed for cases (a–g) is not significant.

To complete the comparison between cases (a–g) the pressure drop for these cases have been calculated and plotted in Fig. 15. The significant difference between pressure drop attainable from using a uniform particle diameter of 1.0 mm and for other cases is very clear in the figure. From Fig. 15, it can be seen that 20–25% savings in the pressure drop can be achieved by using ascending cubic particle diameter distribution with a reduction less than 1.0% in the total mass adsorbed (Fig. 14). Also, for more savings in the pressure drop, the parabolic particle diameter distribution can be used and it should be noted that the reduction in total mass of water adsorbed due to replacing the uniform particle diameter distribution with parabolic descending one (Fig. 14) is small when compared with the savings in the pressure drop due to this modification, as shown in Fig. 15. Also, it should be noted that for descending and ascending linear distribution the pressure drop is the same, on the other hand, the pressure drop for ascending parabolic distribution is higher than that of descending parabolic one. Therefore, it can be recommended that, the uniform particle diameter of 1.0 mm can be replaced with that of cubic or parabolic ascending distributions which will result in a significant reduction in the pressure drop especially in the weakly utilized layers of the bed but however, there would be a slight decrease in the total mass adsorbed. Also, the case of uniform particle diameter of 10.0 mm can be replaced with one of linear and parabolic descending distributions which will increase the available area for heat and mass transfer at the trailing layers of the bed, consequently, the utilization of the trailing layers of the bed is increased as shown in Fig. 16 which shows the axial distribution of water content in the bed after adsorption process, for the cases of uniform particle diameter of 10.0 mm, linear descending and parabolic descending distributions. From Fig. 16 it can be shown that the bed adsorptivity has been enhanced in the trailing layers when smaller particles are used in these layers. Moreover, from Fig. 15 it can be stated that the pressure drop

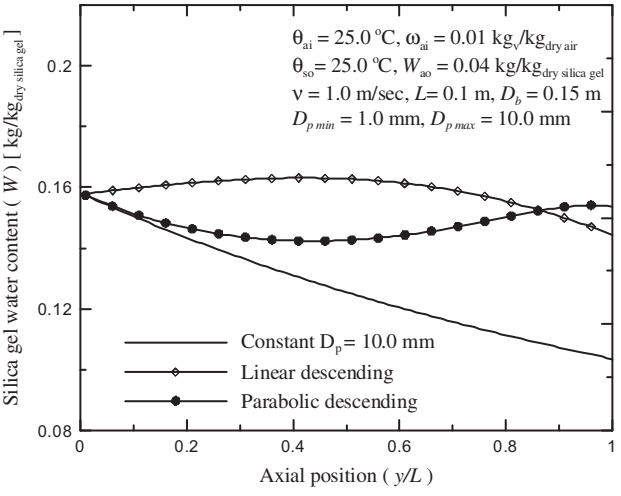

Fig. 16 – Axial distribution of silica gel water content (W) at the end of adsorption process for beds of uniform particle diameter and beds of varying particle diameter at flow velocity (1.0 m s^{-1}).

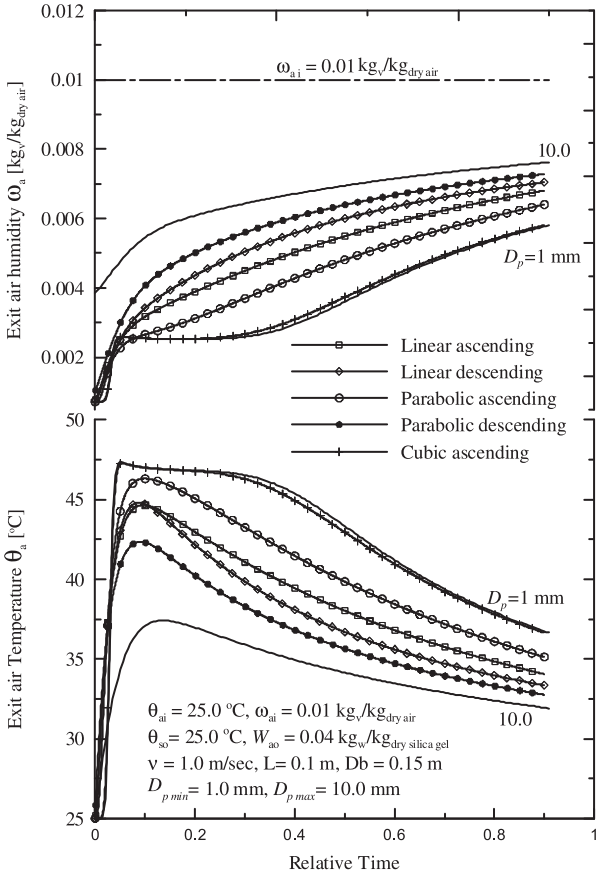

Fig. 17 – Transient variation of exit air humidity ratio and temperature for adsorption process using desiccant beds of uniform particle diameter and beds of varying particle diameter at flow velocity (1.0 m s^{-1}).

increase (from 600 Pa to about 1400 Pa) due to use of smaller particles in the trailing layers can be accepted for enhancing the utilization of the trailing layers as shown in Fig. 16.

Moreover, the cases of higher order particle diameter distributions ($k = 4,5\ldots$) and descending cubic distribution have been tested theoretically, but no difference in the bed performance has been found from that when a uniform particle diameter distribution is used. So, these cases have not been included during this discussion. Fig. 17 shows the transient exit air humidity and temperature for the cases (a–g) during adsorption process. It can be seen that the exit air condition using cubic ascending distribution is the same of that of uniform particle diameter of 1.0 mm then comes the parabolic and linear ascending distributions. And the exit air condition when parabolic descending distribution is used is the nearest to that of uniform particle diameter of 10.0 mm.

7. Conclusions

The heat and mass transfer in a desiccant packed bed of spherical particles has been modeled using a PGC-model and considering the axial heat transfer by conduction in the bed. The developed model has been validated through a comparison with the experimental data from literature for both adsorption and desorption processes, and a good agreement has been found with a maximum root mean square of errors of 3% and 2% for exit air temperature and exit air humidity ratio, respectively. Moreover, the pressure drop in the bed has been calculated using Ergun's equation for different particle diameters and air flow velocities. The effect of particle diameter on the bed performance (adsorption capacity and pressure drop) has been investigated. It has been found that using smaller desiccant particle diameter increases the adsorption capacity. For example, for air velocity of 1.0 m s^{-1}, the total adsorbed mass of water increased from 125 g to 245 g when particles of 10 mm diameter are replaced with particles of 1.0 mm diameter. However, this increase is not significant for flow velocity less than 0.25 m s^{-1} as shown in Fig. 11. An optimization figure for increasing the total mass adsorbed using smaller particle diameter and keeping the minimum increase in pressure drop has been proposed in Fig. 12.

The newly proposed bed of varying particle diameter along the axial direction of bed has been investigated using the validated numerical model. The improvement in the total mass adsorbed and or pressure drop decrease have been investigated for various cases namely, uniform particle diameter, linear ascending, linear descending, parabolic ascending and parabolic descending distributions in the bed. From these investigations the following conclusions are drawn;

1. Replacing the commonly used packed bed of uniform particle diameter of (D_p = 1.0 mm) with the proposed packed bed of cubic particle diameter distribution achieves about 25% reduction in the pressure drop which is translated to savings in the required blowing power with a negligible reduction in the total mass adsorbed (less than 1.0%).
2. It has been found that, for air flow velocity less than 0.25 m s^{-1}, the total mass adsorbed becomes independent of the type of particle distributions in the bed. Moreover, for velocities more than 0.25 m s^{-1}, cubic ascending type particle distribution shows the highest total mass adsorbed when compared to parabolic ascending, linear ascending, linear descending and parabolic descending distributions respectively.
3. However, replacing the bed of uniform particles of 10.0 mm diameter with a bed of linear descending particle diameter distribution, the pressure drop in the bed increases from 750 Pa to 1900 Pa for air velocity of 1.0 m s^{-1}. It also considerably increases total mass adsorbed by about 49% which is more valuable than the increase in the pressure drop. Moreover, the proposed particle diameter distributions enhances the utilization of the trailing layers of the desiccant bed by increasing the water content of the particles by about 50% for the case examined as shown in Fig. 16.

REFERENCES

Anderson, Jan Y., Bjurstrom, Henrik, Azoulay, Michel, Carlson, Bo, 1985. Experimental and theoretical investigation of the kinetics of the sorption of water vapor by silica gel. J. Chem. Soc. Faraday Trans. I 81, 2681–2692.

Awad, M.M., Ramzy, K.A., Hamed, M.A., Bekheit, M.M., 2008. Theoretical and experimental investigation on the radial flow desiccant dehumidification bed. Appl. Therm. Eng. 28, 75–85.

Bjurstrom, Henrik, Karawacki, Ernest, Carlsson, Bo, 1984. Thermal conductivity of a microporous particulate medium: moist silica gel. Int. J. Heat Mass Tran. 27, 2025–2036.

Chakraborty, Anutosh, Saha, Bidyut Baran, Koyama, Shigeru, Kim, Choon Ng, Srinivasan, Kandadai, 2009. Adsorption thermodynamics of silica gel-water systems. J. Chem. Eng. Data 54, 448–452.

Chang, Kuei-Sen, Chen, Mai-Tzu, Chung, Tsair-Wang, 2005. Effects of the thickness and particle size of silica gel on the heat and mass transfer performance of a silica gel-coated bed for air-conditioning adsorption systems. Appl. Therm. Eng. 25, 2330–2340.

Chua, Hui T., Ng Kim, C., Chakraborty, Anutosh, Oo Nay, M., Othman, Mohamed A., 2002. Adsorption characteristics of silica gel+water systems. J. Chem. Eng. Data 47, 1177–1181.

Chung, Jae Dong, Lee, Dae-Young, 2009. Effect of desiccant isotherm on the performance of desiccant wheel. Int. J. Refrigeration 32, 720–726.

Elsayed, S.S., Miyazakia, T., Hamamoto, Y., Akisawa, A., Kashiwagi, T., 2008. Performance analysis of air cycle refrigerator integrated desiccant system for cooling and dehumidifying warehouse. Int. J. Refrigeration 31, 189–196.

Farooq, Shamsuzzaman, Ruthven, Douglas M., 1990. Heat effects in adsorption column dynamics. I. Comparison of one and two-dimensional models. Ind. Eng. Chem. Res. 29, 1076–1084.

Gurgel, J.M., Filho Andrade, L.S., Grenier, Ph., Meunier, F., 2001. Thermal diffusivity and adsorption kinetics of silica-gel/water. Adsorption 7, 211–219.

Hamed, Ahmed M., Abd El Rahman, Walaa R., El-Eman, S.H., 2010. Experimental study of the transient adsorption/desorption characteristics of silica gel particles in fluidized bed. Energy 35, 2468–2483.

Heidarinejad, Ghassem, Pasdarshahri, Hadi, 2011. Potential of a desiccant-evaporative cooling system performance in a multi-climate country. Int. J. Refrigeration 34, 1251–1261.

Incropera, Dewitt, Bergman, Lavine, 2007. Fundamentals of Heat and Mass Transfer, sixth ed. Wiley, New York, pp. 941–942.

Jeong, Jongsoo, Yamaguchi, Seiichi, Saito, Kiyoshi, Kawai, Sunao, 2010. Performance analysis of four-partition desiccant wheel and hybrid dehumidification air-conditioning system. Int. J. Refrigeration 33, 496–509.

Jeong, Jongsoo, Yamaguchi, Seiichi, Saito, Kiyoshi, Kawai, Sunao, 2011. Performance analysis of desiccant dehumidification systems driven by low-grade heat source. Int. J. Refrigeration 34, 928–945.

Jia, C.X., Dai, Y.J., Wu, J.Y., Wang, R.Z., 2007. Use of compound desiccant to develop high performance desiccant cooling system. Int. J. Refrigeration 30, 345–353.

Kafui, K.D., 1994. Transient heat and moisture transfer in thin silica gel beds. Trans. ASME – J. Heat Tran. 116, 946–953.

Kim, Min-Bae, Moon, Jong-Ho, Lee, Chang-Ha, Ahn, Hyungwoong, Cho, Wonihl, 2004. Effect of heat transfer on the transient dynamics of temperature swing adsorption process. Korean J. Chem. Eng. 21, 703–711.

Kluson, P., Scaife, S., Quirke, N., 2000. The design of micro-porous graphitic adsorbents for selective separation of gases. Sep. Purif. Technol. 20, 15–24.

Liu, Y.L., Wang, R.Z., Xia, Z.Z., 2005. Experimental study on a continuous adsorption water chiller with novel design. Int. J. Refrigeration 28, 218–230.

Maggio, G., Freni, A., Restuccia, G., 2006. A dynamic model of heat and mass transfer in a double-bed adsorption machine with internal heat recovery. Int. J. Refrigeration 29, 589–600.

Majumdar, Pradip, 1998. Heat and mass transfer in composite desiccant pore structure for dehumidification. Sol. Energy 62, 1–10.

Meyer, Oscar A., Weber, Thomas W., 1967. Nonisothermal adsorption in fixed beds. AIChE J. 13, 457–465.

Miyazaki, Takahiko, Akisawa, Atsushi, Saha, Bidyut Baran, 2010. The performance analysis of a novel dual evaporator type three-bed adsorption chiller. Int. J. Refrigeration 33, 276–285.

Mutlu, Mehmet, Gökmen, Vural, 1998. Determination of effective mass transfer coefficient (Kc) of patulin adsorption on activated carbon packed bed columns with recycling. J. Food Eng. 35, 259–266.

Ng, K.C., Chua, H.T., Chung, C.Y., Loke, C.H., Kashiwagi, T., Akisawa, A., Saha, B.B., 2001. Experimental investigation of the silica gel-water adsorption isotherm characteristics. Appl. Therm. Eng. 21, 1631–1642.

Pesaran, Ahmad A., Mills, Anthony F., 1987a. Moisture transport in silica gel packed beds I-theoretical study. Int. J. Heat Mass Tran. 30, 1037–1049.

Pesaran, Ahmad A., Mills, Anthony F., 1987b. Moisture transport in silica gel packed beds-II. Experimental study. Int. J. Heat Mass Tran. 30, 1051–1060.

Rady, M.A., Huzayyin, A.S., Arquis, E., Monneyron, P., Lebot, C., Palomo, E., 2009. Study of heat and mass transfer in a dehumidifying desiccant bed with macro-encapsulated phase change materials. Renew. Energy 34, 718–726.

Ramzy, A.K., Kadoli, R., Ashok Babu, T.P., 2011. Improved utilization of desiccant material in packed bed dehumidifier using composite particles. Renew. Energy 36, 732–742.

Ruivo, C.R., Costa, J.J., Figueiredo, A.R., 2011. Influence of the atmospheric pressure on the mass transfer rate of desiccant wheels. Int. J. Refrigeration 34, 707–718.

San, Jung-Yang, Hsu, Yuh-Ching, Wu, Liang-Jen, 1998. Adsorption of toluene on activated carbon in a packed bed. Int. J. Heat Mass Tran. 41, 3229–3238.

San, Jung-Yang, Jiang, Gwo-Dong, 1994. Modeling and testing of a silica gel packed bed system. Int. J. Heat Mass Tran. 37, 1173–1179.

Sircar, Shivaji, 2006. Removal of heat of adsorption from adsorbent by forced convection. Adsorption 12, 167–174.

Sodre, J.R., Parise, J.A.R., 1998. Fluid flow pressure drop through an annular bed of spheres with wall effects. Exp. Therm. Fluid Sci. 17, 265–275.

Sun, Jin, Besant, Robert W., 2005. Heat and mass transfer during silica gel–moisture interactions. Int. J. Heat Mass Tran. 48, 4953–4962.

Wang, Xiaolin, Chua, H.T., 2007. Two bed silica gel-water adsorption chillers: an effectual lumped parameter model. Int. J. Refrigeration 30, 1417–1426.

Weixing, Yuan, Yi, Zheng, Xiaoru, Liu, Xiugan, Yuan, 2008. Study of a new modified cross-cooled compact solid desiccant dehumidifier. Appl. Therm. Eng. 28, 2257–2266.

White, Stephen D., Goldsworthy, Mark, Reece, Roger, Spillmann, Thorsten, Gorur, Abdullah, Lee, Dae-Young, 2011. Characterization of desiccant wheels with alternative materials at low regeneration temperatures. Int. J. Refrigeration. doi:10.1016/j.ijrefrig.2011.06.012.